

See discussions, stats, and author profiles for this publication at: <https://www.researchgate.net/publication/233841501>

Mapping atmospheric corrosion in coastal regions: methods and results

Data · December 2012

CITATIONS

16

READS

28,342

17 authors, including:



Rudolf Brázdil

Masaryk University

361 PUBLICATIONS 12,244 CITATIONS

SEE PROFILE



Rüdiger Glaser

University of Freiburg

426 PUBLICATIONS 5,623 CITATIONS

SEE PROFILE



Christian Pfister

University of Bern

237 PUBLICATIONS 9,331 CITATIONS

SEE PROFILE



Petr Dobrovolny

Masaryk University

174 PUBLICATIONS 5,750 CITATIONS

SEE PROFILE

Journal of Photonics for Energy

SPIDigitalLibrary.org/jpe

Mapping atmospheric corrosion in coastal regions: methods and results

Karolina Slamova
Rüdiger Glaser
Christian Schill
Stefan Wiesmeier
Michael Köhl

Mapping atmospheric corrosion in coastal regions: methods and results

Karolina Slamova,^a Rüdiger Glaser,^b Christian Schill,^a Stefan Wiesmeier,^a
and Michael Köhl^a

^aFraunhofer Institute for Solar Energy Systems ISE, Div. PV-Modules and Reliability,
Heidenhofstr. 2, 79110 Freiburg, Germany
karolina.slamova@ise.fraunhofer.de

^bUniversity of Freiburg, Institute of Physical Geography, Werthmannstr. 4, 79098 Freiburg,
Germany

Abstract. Corrosion can seriously affect the service life of components for solar energy conversion. We present results of mapping the potential of atmospheric corrosion in coastal regions with the aid of a Geographical Information System (GIS). Concentration of sea salt aerosols, which are the main atmospheric pollutants in maritime coastal regions, gives an indication of the probability of the atmospheric corrosion leading to PV-module degradation. Two approaches to estimate the distribution of sea salt aerosol across the coastal regions worldwide are investigated. The first approach is a geo-statistical analysis that has been used for interpolating chloride deposition data. The second approach is based on modeling the environmental conditions, which are affecting source and distribution of airborne salinity. The comparison of these two approaches provides high accuracy in the description of the variation in airborne salinity across the coastal regions. The assessment of the atmospheric corrosion in coastal regions is based on the international standard ISO 9223. The corrosivity classification is simply defined by three parameters: SO₂ pollution, airborne salinity, and relative humidity. A combination of the results from the geo-statistical approach and modeling is used; the result is a map of atmospheric corrosion in coastal regions. © 2012 Society of Photo-Optical Instrumentation Engineers (SPIE). [DOI: [10.1117/1.JPE.2.022003](https://doi.org/10.1117/1.JPE.2.022003)]

Keywords: sea salt aerosol; atmospheric corrosion; corrosivity mapping; modeling; geographical information system; geo-statistical methods.

Paper 12003SS received Jan. 13, 2012; revised manuscript received May 25, 2012; accepted for publication Jun. 4, 2012; published online Jun. 29, 2012.

1 Introduction

Solar power systems are naturally exposed to weathering. Local load factors like temperature, relative humidity, irradiation (especially ultraviolet (UV) radiation), and atmospheric corrosion have a negative influence on quality and service life of the materials. Atmospheric corrosion is reported to account for more failures in terms of cost than any other factor¹ and is the main contributor to the overall costs of corrosion in general. These are estimated to be in the range of 2% to 4% of the gross national product for several countries.² In the solar sector atmospheric corrosion is a typical module degradation mechanism. Corrosion attacks cell metallization in crystalline silicon modules and semiconductor layers in thin-film modules, causing loss of electrical performance.³

Atmospheric corrosion varies significantly in different environments. There are coastal regions particularly suited for solar power systems because of their high density of population⁴ and high solar radiation⁵—especially in regions at lower latitudes. Unfortunately their marine atmosphere is highly corrosive.⁶ Fine wind-swept chloride particles deposited on surfaces characterize this type of atmosphere.² These atmospheric pollutants are produced both in the open ocean and by the breaking surf as droplets or crystals and transported towards the land.⁷

The salinity data are usually obtained by using the wet candle method gauging a chloride deposition rate, which is expressed in milligrams per square meter per day ($\text{mgCl}/\text{m}^2/\text{d}$).⁸

The chloride deposition usually decreases strongly with increasing distance from the shore in marine environments, as the droplets and crystals settle by gravitation or may be filtered off when the wind passes through vegetation.⁹

Atmospheric salinity influences the process of atmospheric corrosion and can cause significant damage to the materials used in photovoltaic modules. However, its role may change depending on climate, because a very humid climate can cause a fast leaching of chloride ions and diminish their effect on the acceleration of the corrosion rate.¹⁰

The next important parameter for estimating atmospheric corrosion, according to the international standard ISO 9223, is the Time of Wetness together with industrial pollutants (SO_2 -Pollution). Although there are many other possible parameters determining atmospheric corrosion, the classification in this international standard uses these three parameters for categorization of the atmospheric corrosion and divides atmospheric corrosion into five categories from C1 to C5 as given in Table 1.¹¹

Information about atmospheric corrosion at potential locations for solar generators is important for the selection of materials and suitable protective coatings. A corrosion map is a useful instrument, as it gives a general indication of the potential atmospheric corrosion in different locations in the world.

This paper presents the results of interpolated and simulated airborne salinity data for the coastal regions in global maps using a geographical information system (GIS). GIS integrates the technologies for acquisition and processing of the spatially distributed data.

Despite detailed work investigating relationships between the measured corrosion rates and climatic parameters, no universal atmospheric corrosion model applicable across a variety of countries and environmental condition could be developed.⁷ Corrosion maps are produced on a regional or national scale mostly, like a German corrosion map from Anshelm¹² or an Australian corrosion map from Cole.⁷ Different simulation models are implemented for the assessment of the conditions at concrete locations. Few national corrosion maps exist using the same classification as presented in the map in Fig. 1. These maps are produced by The National Association of Corrosion Engineers (NACE) and the corrosion data are derived from different research projects in the field of atmospheric corrosion.

The airborne salinity is the essential factor determining atmospheric corrosion in marine regions.¹⁴ Previously published methods for modeling airborne salinity, such as those by Meira¹⁵ or Guan,¹⁶ were restricted to small areas and analyze local environmental conditions only. Often there is not only one model but combinations of different models describing the process of the generation and transport of sea salt aerosols.

For example, the holistic model described by Cole⁷ for predicting airborne salinity consists, in fact, of four models: the production of aerosols by surf, the production of aerosols by the ocean, the transport of surf-produced aerosols, and the transport of ocean-produced aerosols. These newly developed models have high accuracy for the concrete sites because they have been adapted to their environmental conditions. But the application of these small-scale models to a global scale will result in considerable errors because of the increasing complexity. Some parameters used in these small-scale models, such as weighted mean wind velocity (v_{mp}) are not available on a global scale.

Table 1 Categories of corrosivity of the atmosphere (referring to Ref. 11).

Category	Corrosivity (C)
C ₁	Very low
C ₂	Low
C ₃	Medium
C ₄	High
C ₅	Very high

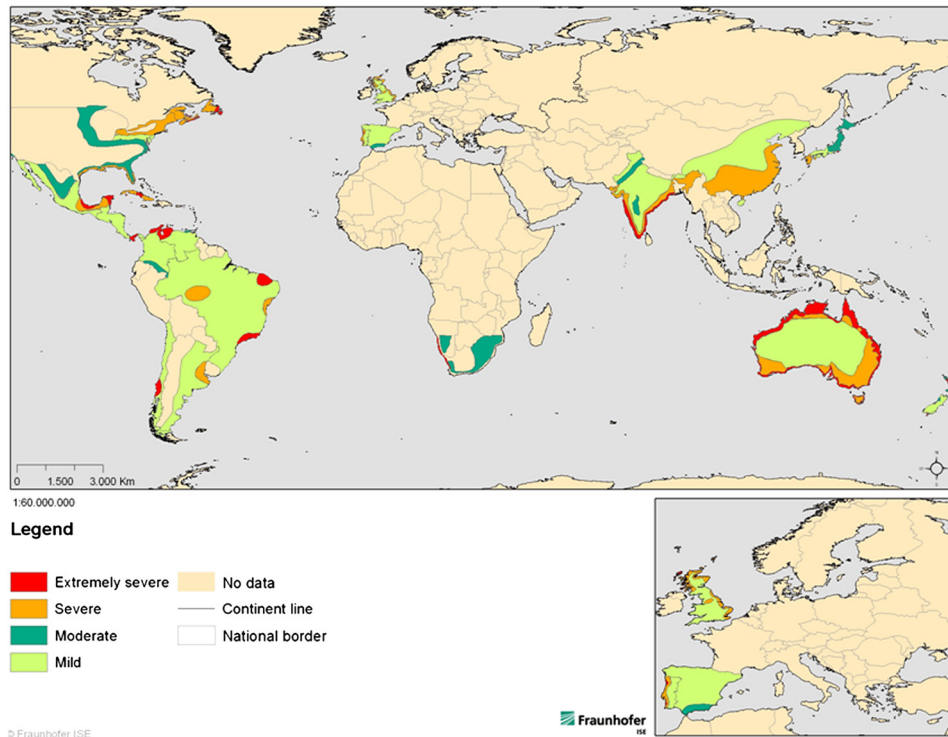


Fig. 1 Distribution of national corrosion data worldwide (referring to NACE¹³).

2 Interpolation Techniques for Airborne Salinity Mapping

The GIS—ArcInfo ArcGIS Desktop—developed by ESRI was used for the mapping of airborne salinity and atmospheric corrosion. For better visualization of results, the coastal regions are displayed as a strip with a maximum distance of 500 km from the sea. Only regions well-suited for solar energy usage are selected, thus the northern parts of Russia and of North America as well as Antarctica are neglected. Only regions with enough chloride deposition data can be used for the mapping of airborne salinity by means of interpolation methods. No airborne salinity data actually exist for the African continent.

Two different approaches to evaluate the airborne salinity in the coastal regions have been applied—interpolation and simulation. Interpolation is used in GIS to predict cell values at locations that lack sampled points. Punctual chloride deposition data in form of annual average data ($\text{mgCl}/\text{m}^2/\text{d}$) have been collected for this approach.

The main part of the chloride deposition data has been taken from the Korrfield database produced by the Swedish institute for corrosion and metals research (Swerea) KIMAB. The rest of the data has been collected from different literature sources. These data from more than 250 measuring stations have been geo-referenced by GIS and the layers have been defined in order to be interpolated by the geo-statistical methods from the ESRI-Spatial Analyst toolbox. Inverse distance weighted (IDW) and a simple Kriging interpolation have been applied for the calculations of grids. IDW determines cell values using a linear-weighted combination set of sample points. The weight assigned is a function of the distance of an input point from the output cell location. The general formula of IDW interpolation according to Li¹⁷ is the following:

$$w(x, y) = \sum_{i=1}^N \lambda_i \cdot w_i, \quad (1)$$

$$\lambda_i = \frac{\left(\frac{1}{d_i}\right)^p}{\sum_{k=1}^N \left(\frac{1}{d_k}\right)^p}, \quad (2)$$

where $w(x, y)$ is the predicted value at location (x, y) , N is the number of nearest known points surrounding (x, y) , λ_i are the weights assigned to each known point value w_i at location (x_i, y_i) , d_i are the Euclidean distances between each (x_i, y_i) and (x, y) , and p is an exponent, which influences weighting of w_i on w .¹⁷

Kriging is a geo-statistical method that uses a statistical technique for predicting values derived from the measure of relationship in samples and employs sophisticated weighted-average techniques.¹⁸ The most commonly applied form of Kriging uses a “semivariogram”—a measure of spatial correlation between pairs of points describing the variance over a distance or lag h . Weights change according to the spatial arrangement of the samples. The linear combination of weights are of the form:

$$\sum y_i \lambda_i, \quad (3)$$

where y_i are the variables evaluated in the observation locations, λ_i are the Kriging weights. The main difference between interpolation using deterministic and statistical methods is that the Kriging prediction is accompanied by an estimated prediction standard error. The semi-variogram is an essential step in determining the spatial variation in the sampled variable. It provides useful information for interpolation, sampling density, determining spatial patterns, and spatial simulation. The semi-variogram is of the form:

$$\gamma(h) = \frac{1}{2} E[y(x) - y(x + h)]^2, \quad (4)$$

where $\gamma(h)$ is semi-variogram dependent on distance or lag h , $(x, x + h)$ is the pair of points with distance vector h , $y(x)$ is a regionalized variable y at point x , $y(x) - y(x + h)$ is the difference of the variable at two points separated by h , and E is mathematical expectation.¹⁹

The results of both different interpolation methods agree well with each other in magnitude as well as in the spatial patterns of areas with high and low airborne salinity. The spatial results produced by IDW are more exact and easily comprehensible than by the Kriging method indicating that in our case the IDW method is more suitable.

The result-grid has been calculated by using the Weighted Overlay tool from the Spatial Analyst in GIS. This tool overlays several raster-datasets using a common measurement scale and weights each layer according to its importance. The final map in Fig. 2 includes the results of both interpolation methods. The airborne salinity is represented by a color index, where the number 9, displayed in red, corresponds to the highest airborne salinity and the number 1, displayed in green, represents the lowest airborne salinity. The sites whose chloride deposition data were used are displayed in the map as well. The size of the symbols represents the measured chloride deposition, which is classified according to ISO 9223. Regions with very high airborne salinity could be found especially in eastern China, the Korean Peninsula, the north-western part of the Arabian Peninsula, and Turkey. On the American continent the regions with high airborne salinity rates are situated in eastern Brazil, the island-states in the Caribbean, and in Florida. High airborne salinity in Europe is found in Greece, in the coastal regions of western France, in the eastern part of Great Britain, and in the northern part of Denmark.

3 Modeling of Airborne Salinity

The second approach to produce an airborne salinity map is the modeling of salt production and transport based on the environmental conditions. There are many factors which can influence airborne salinity. The frequency and intensity of cyclonic activity in terrestrial mid-latitudes affect the main part of the global generation and distribution of marine aerosols. Other factors, such as relief, wind speed and intensity, vegetative cover, closeness to cities and industrial centers, mining facilities, etc. can act at regional or local scales, modifying the local deposition of salt. For the modeling of the airborne salinity in our study, the environmental input parameters

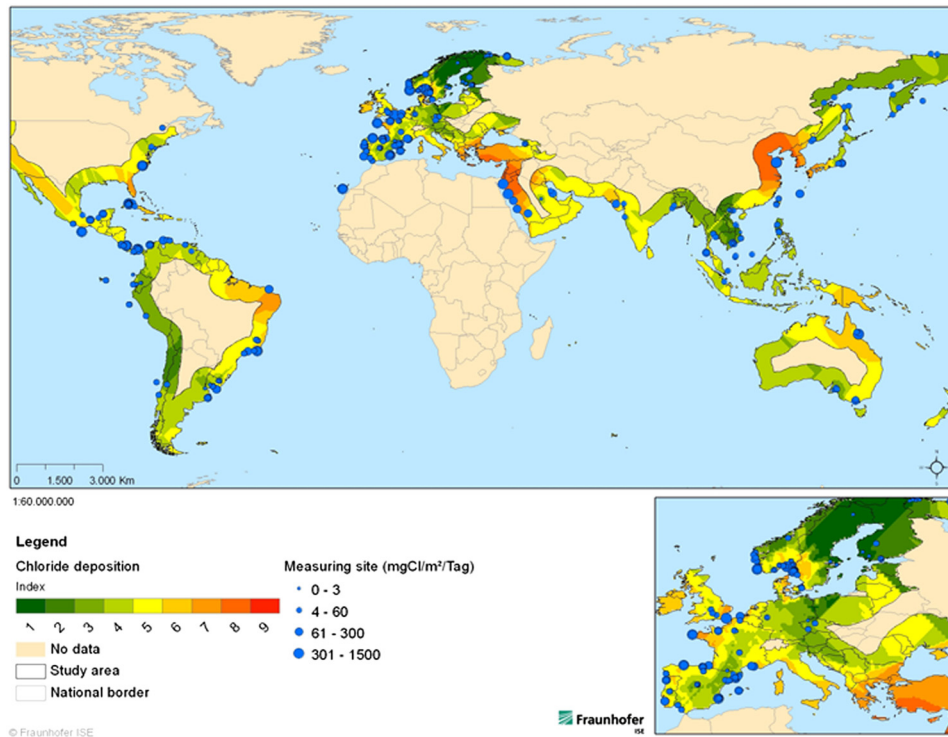


Fig. 2 Map of airborne salinity in the coastal regions worldwide.

Table 2 Inputs parameters used for salinity modeling.

Parameters	Organisation	Units	Year
Climatic			
Relative humidity	The Atlas of the Biosphere	[%]	1961–1990
Wind speed	SWERA	[m/s]	2005
Wind direction	NASA	[degree]	1983–1993
Mean annual amount of precipitation	WorldClim	[mm]	1950–2000
Environmental			
Ocean salinity	NOAA	[g/l]	2009
Altitude	WorldClim	[m]	2000
Land cover	ESA		2005–2006

are: precipitation, land cover, relative humidity (RH), elevation, wind speed, wind direction, and ocean salinity (Table 2).

The salt particles can be easily dissolved in raindrops or fog droplets. Rain tends to wash out the salt particles from the atmosphere. Salt particles not associated with fog or rain can be captured by wetted vegetation. The drier the vegetation and the lower the humidity of the ambient air, the further the transport of salt particles will be. Transport of salt particles is also affected by land surface roughness.²⁰ The influence of ground roughness on salt concentration is strongest in the first hundred meters from the sea.²¹ In the ocean, the wind speed and ocean salinity have the most influence on high airborne salinity. Wind characteristics strongly affect the production of marine aerosols. There is an exponential increase of salt concentration with wind speed.¹⁵

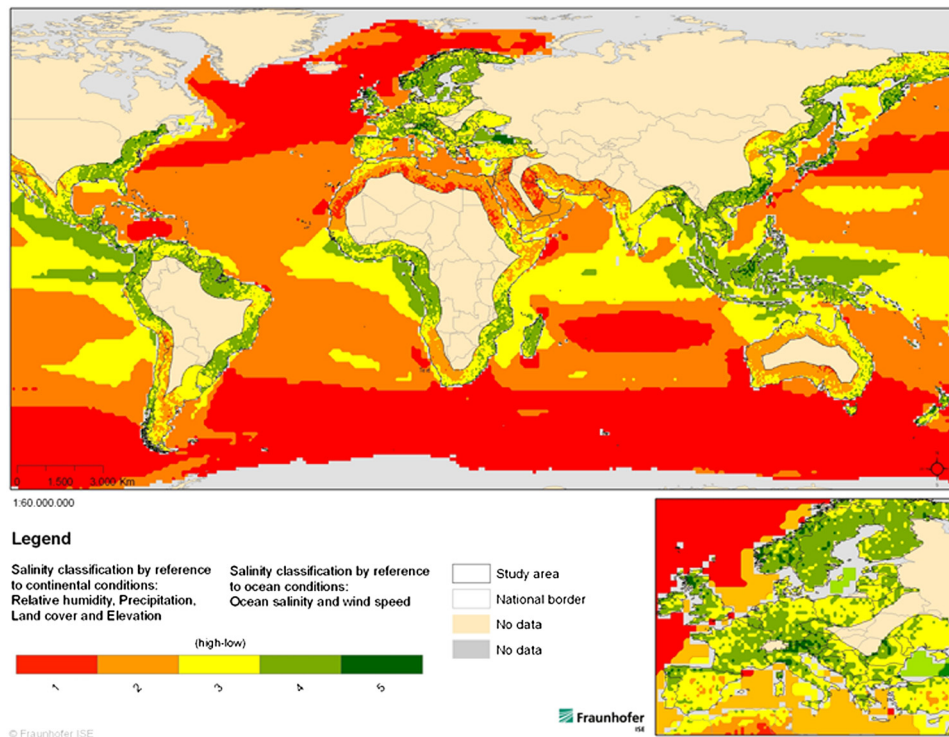


Fig. 3 Classification of airborne salinity by reference to continental and ocean conditions.

Ocean salinity is particularly important for the production of marine aerosols. The higher the ocean salinity, the higher is the chloride concentration in the precipitation.²² A data set for one year has been used for modeling. First a grid for the continental conditions for airborne salinity in the coastal regions (relative humidity, annual precipitation, altitude, and land cover) using the weighted overlay tool has been calculated. The ocean conditions have been calculated from wind speed and ocean salinity. The map in the Fig. 3 presents results of the simulation of the environmental conditions which affect airborne salinity. The map shows the interaction of the continental and sea conditions and allows an overview of the coastal regions that are most affected by high airborne salinity and consequently also by high atmospheric corrosion.

The regions with high continental airborne salinity are marked in red on the map like the sites with high airborne salinity in the ocean. The essential parameter affecting airborne salinity wind direction is not included in this map.²³ An increase in wind speed does not always lead to an increase in airborne salinity, as the final result is dependent on the wind direction.

The marine wind directions contribute most to the entrainment of marine aerosols from the sea towards the land.²³ Figure 4 shows the results of the simulation, which combines all continental and ocean conditions in the coastal regions influencing airborne salinity and adds the factor wind direction. The map displays the summer wind situation (on the northern hemisphere) using data from August. The wind direction is divided in 9 segments of 40 deg. It allows identification of the regions with favorable conditions for high airborne salinity because of the dominantly sea-side direction of the wind. The interaction of all these parameters causes high airborne salinity and therefore severe corrosion potential.

4 Comparison

The results of mapping of the actual airborne salinity using the interpolation approach correspond well with the results of the modeling approach. The maps (Figs. 2 and 4) have very good conformity for the regions in Central and South America. The regions with high airborne salinity could be found in the east part of Brazil and in the Caribbean island countries in both of the maps. In Australia there are high salinity-affected regions at the north and north-west coast.

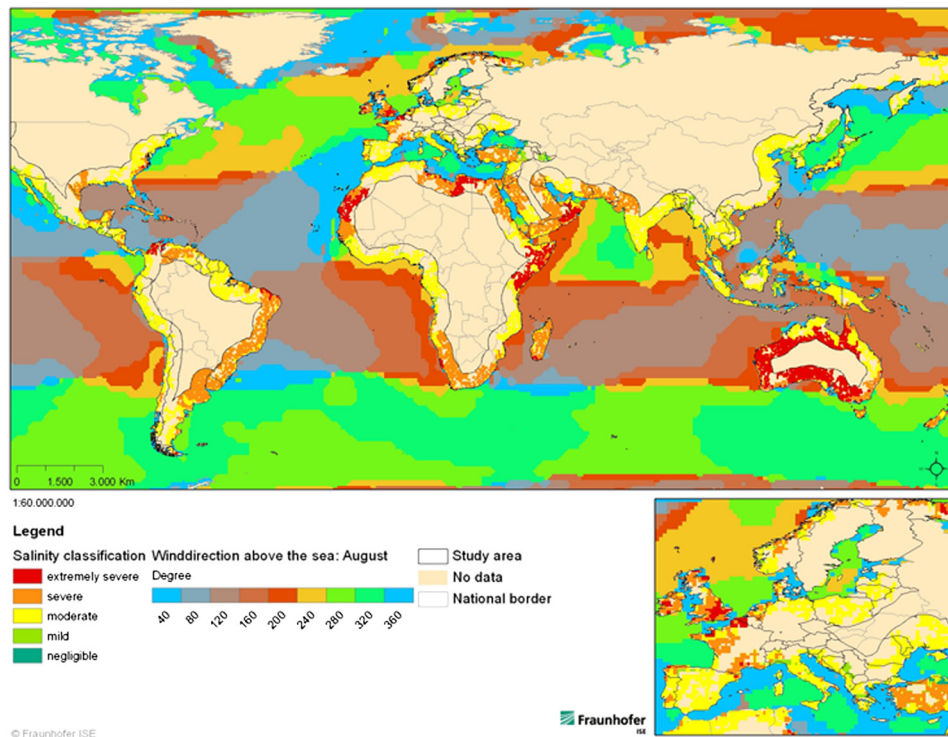


Fig. 4 Airborne salinity classification including the wind condition for the summer climatic situation.

Moreover, the regions on the Arabian Peninsula feature high airborne salinity in the maps of both of the methods, but the geographical distribution is partly different.

The interpolation method resulted in high airborne salinity rates in the coastal regions of west France, in the east part of Great Britain, and in the north part of Denmark. These results could also be found on the map resulting from modeling. The results for Greece, Bulgaria, and regions of East Asia do not agree very well. While the regions in eastern China and on the Korean peninsula show high airborne salinity in the interpolation map, only moderate airborne salinity was resulting from modeling.

The interpolation of spatial data by using IDW and Kriging is well applicable for estimating airborne salinity as well as using the modeling of the environmental conditions to obtain the airborne salinity map. The disparities can be caused by the nonuniform distribution of the measuring points on the global map leading to overestimation or underestimation by the interpolation method. The spatial accuracy will be higher by using more measuring points. Some disagreement between the results could be caused by the modeling of the environmental conditions too. The spatial details of the map depend strongly on the availability of climatic and geographic data.

Using global raster data lead to good results on the global scale, which can get a good overview of the problematic situations. Higher temporal and spatial resolution of the raster data is essential for the analysis of local differences of the airborne salinity. Also, the global wind conditions should be taken into account more for the modeling of airborne salinity.

5 Corrosivity Mapping

A corrosion rate is determined by atmospheric pollution and time of wetness as the international standard ISO 9223¹¹ describes. This standard is used by many studies on corrosion mapping. Sica uses the classification in this standard to determine the atmospheric corrosion in the North Brazilian Coast.²⁴

However, he concentrates on a small research area and models the corrosions factors on the local scale. Here a new method based on ISO 9223 for estimating atmospheric corrosion is developed. In our study, atmospheric pollution is divided into two categories: pollution by

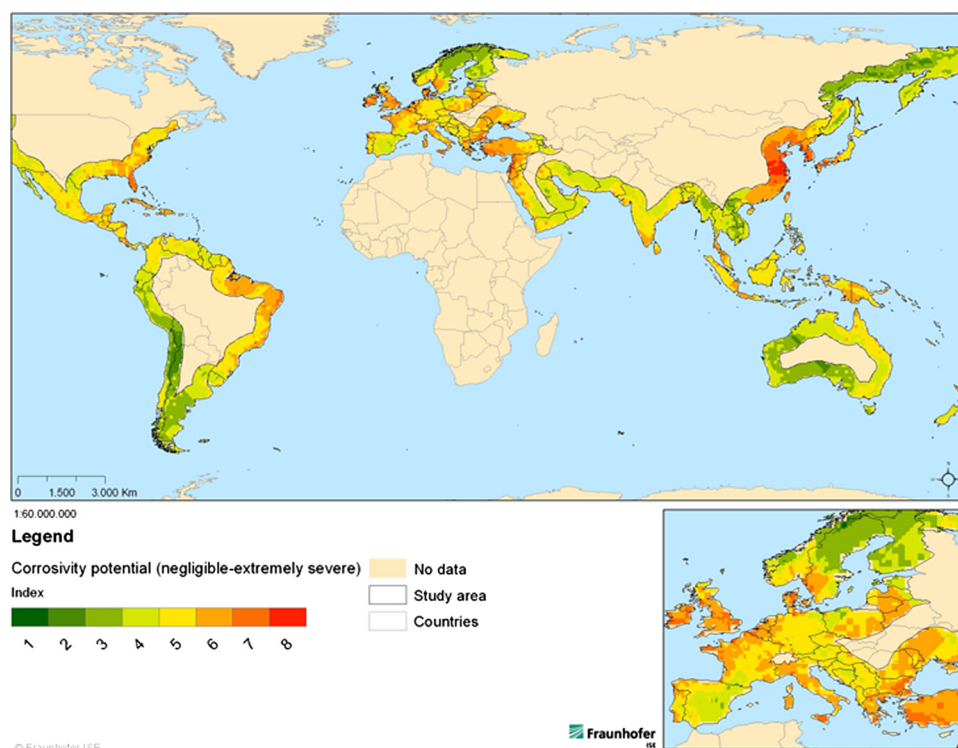


Fig. 5 Distribution of atmospheric corrosivity on the global map—final results of GIS-analyst.

sulphur dioxide from anthropogenic sources [derived from data from United Nations Environment Programme (UNEP)] and pollution by airborne salinity represented by chloride deposition raster. The Weighted Overlay tool in GIS has been applied as a main instrument to compare these two raster data with relative humidity raster.

The biggest attention has been given to airborne salinity, because it plays a key role in atmospheric corrosion in coastal regions. Therefore the airborne salinity-raster was given the biggest weighting factor of 50%. Relative humidity is affecting the atmospheric corrosion, because an aqueous electrolyte film is formed on the metal surfaces in humid environments, which is necessary for a corrosion reaction. Relative humidity substitutes the parameter time of wetness from the international standard ISO 9223, because the parameter time of wetness is not available as a global raster. The relative humidity raster was assigned a weighting factor of 30%. SO_2 emission is the last parameter for the evaluation of atmospheric corrosion. Because SO_2 emissions are mainly produced by combustion as a result of oxidation of sulphur, high rates of SO_2 are expected in urban or industrial regions in China or Europe.²⁵ The weighting factor for SO_2 emission has been set to 20%. According to these conditions, the map estimating rate of atmospheric corrosion in the coastal regions has been created and is shown in Fig. 5.

The atmospheric corrosion in the coastal regions is classified in 8 groups according to the three key corrosion factors: RH, airborne salinity, and sulphur dioxide pollution levels.

Category 8 is plotted with dark red color and means extremely high corrosion rate; the regions in category 1 (green) have very mild atmospheric corrosion. However, coastal regions in classes 7 or 6 still have high corrosion rates too. On the global map it can be seen that in the coastal regions of China and Brazil, the east coast of USA, in Central American states, on the Arabian Peninsula, and in Turkey high atmospheric corrosion can be found. High atmospheric corrosion in these regions is caused either by very high airborne salinity (such as on the Arabian Peninsula) or by interaction of all three main factors.

East China with its high atmospheric corrosion rates is a good example of the second situation. High rates of airborne salinity together with high RH and high rates of SO_2 -emissions cause high atmospheric corrosion in these regions. In Europe the atmospheric corrosion is high compared to other coastal regions. Atmospheric corrosion categories 6 and 7 apply to Great Britain, the north and east coast of France, Belgium, the Netherlands, Denmark, and southern Sweden.

The high rates of atmospheric corrosion in these regions are mainly caused by the interaction of all three main factors.

6 Conclusion

The global corrosion rates were estimated by using a Geographical Information System, which integrates the techniques for acquisition and processing of the spatially distributed data, taking into account the influence of the main corrosion factors: airborne salinity, high atmospheric humidity, and emission of SO₂.

With GIS it is possible to combine these different types of data and to present them as a resulting corrosivity map. The values of the airborne salinity data can be estimated at sites where no samples are available by either using interpolation methods or by simulation using suitable models.

The information about spatial distribution of atmospheric corrosion on the world map can be used as a reference for the selection of materials in solar energy systems. Further work will focus on the extension of the stress mapping to other degradation factors like UV-radiation and the expected sample temperatures, as well as the surface humidity levels in order to provide tools for the design of stress tests as a function of the location or the definition of stress categories for the design of appropriate solar components with sufficient durability.

Acknowledgments

The work was partly funded by the German Federal Ministry for the Environment, Nature Conservation and Nuclear Safety (BMU FKz 0329978), and sponsored by the industrial partners Scheuten Solar, Schott Solar, Solarfabrik, Solarwatt, SolarWorld, and Solon.

References

1. S. L. Pohlmann, "Atmospheric corrosion," in *ASM Handbook*, J. R. Davis, Ed., pp. 80–83, ASM International, Material Park, OH (1987).
2. M. Tullmin and P. R. Roberge, "Atmospheric corrosion," in *Uhling's Corrosion Handbook*, R. Winston Revie Ed., pp. 305–321, A Wiley-Interscience Publication, Ottawa, Canada (2000).
3. M. A. Quintana and D. L. King, "Commonly observed degradation in field-aged photovoltaic modules," in *Proc. of the 29th Specialist Conference, IEEE PVSC, 2002*, New Orleans, LA (2002).
4. Eurostat Regional Yearbook 2010, Publication of the European Union, Luxembourg (2010).
5. Meteonorm, "Global Radiation Europe (long term mean 1986-2005)," <http://www.meteonorm.com/pages/de/meteonorm.php?lang=DE> (27 April 2011).
6. M. Morcillo et al., "Atmospheric corrosion of copper in Ibero-America," *Corrosion* **57**(11), 967–980 (2001), <http://dx.doi.org/10.5006/1.3290321>.
7. I. S. Cole et al., "Multi-scale modeling of the corrosion of metals under atmospheric corrosion," *Mater. Sci. Forum* **561–565**, 2209–2212 (2007), <http://dx.doi.org/10.4028/www.scientific.net/MSF.561-565>.
8. *ISO 9225: Corrosion of Metals and Alloys—Corrosivity of Atmospheres—Measurement of Pollution*, ISO, Geneva, Switzerland (1992).
9. A. I. Almarshad and S. Syed, "Atmospheric corrosion of galvanized steel and aluminium in marine and marine-industrial environments of Saudi Arabia," *Mater. Corros.* **59**(1), 46–51 (2008), [http://dx.doi.org/10.1002/\(ISSN\)1521-4176](http://dx.doi.org/10.1002/(ISSN)1521-4176).
10. F. Corvo et al., "Atmospheric corrosivity in the Caribbean area," *Corros. Sci.* **39**(5), 823–833 (1997), [http://dx.doi.org/10.1016/S0010-938X\(96\)00138-2](http://dx.doi.org/10.1016/S0010-938X(96)00138-2).
11. *ISO: 9223: Corrosion of Metals and Alloys—Corrosivity of Atmospheres—Classification*, ISO, Geneva, Switzerland (1992).
12. F. Anshelm et al., "Mapping actual corrosion rates and exceedances of acceptable corrosion rates. Procedure and results," in *Proc. of a UNECE Workshop*, Stockholm, Sweden, pp. 27–40 (2000).

13. NACE, "Corrosion and Pollution," Available at <http://events.nace.org/library/corrosion/AtmCorros/mapNA.asp> (29 April 2011).
14. R. T. Vashi and H. K. Kadiya, "Corrosion study of metal in marine environment," *E-J. Chem.* **6**(4), 1240–1246 (2009), <http://dx.doi.org/10.1155/2009/509216>
15. G. R. Meira et al., "Modeling sea-salt transport and deposition in marine atmosphere zone—a tool for corrosion studies," *Corros. Sci.* **50**(9), 2724–2731 (2008), <http://dx.doi.org/10.1016/j.corsci.2008.06.028>.
16. H. Guan et al., "Factors influencing chloride deposition in a coastal hilly area and application to chloride deposition mapping," *Hydrol. Earth Syst. Sci.* **14**(5), 801–813 (2010), <http://dx.doi.org/10.5194/hess-14-801-2010>.
17. L. Li, "Constraint database and data interpolation," in *Encyclopedia of GIS*, S. Shekhar and H. Xiong, Eds., pp. 144–153, Springer Science + Business Media, New York (2008).
18. C. Childs, "Interpolating surfaces in ArcGIS spatial analyst," *Arc User: The Magazine for Esri Software Users—Return on Investment*, July–September, 32–35 (2004) <http://www.esri.com/news/arcuser/0704/summer2004.html> (27 April 2011).
19. A. D. Hartkamp et al., "Interpolation techniques for climate variables," NRG-GIS Series 99-01, CIMMYT, Mexico, D.F. (1999).
20. G. R. Meira et al., "Measurements and modeling of marine salt transportation and deposition in a tropical region in Brazil," *Atmos. Environ.* **40**(29), 5596–5607 (2006), <http://dx.doi.org/10.1016/j.atmosenv.2006.04.053>.
21. I. S. Cole, D. A. Paterson, and W. D. Ganther, "Holistic model for atmospheric corrosion part 1—theoretical framework for production, transportation and deposition of marine salts," *Corros. Eng. Sci. Technol.* **38**(2), 129–134 (2003), <http://dx.doi.org/10.1179/147842203767789203>.
22. Deutscher Wetterdienst, Gutachten über den Salzgehalt der Luft in Meeresnähe. Meteorologisches Observatorium Hamburg (1990).
23. M. Morcillo et al., "Salinity in marine atmospheric corrosion: its dependence on the wind regime existing in the site," *Corros. Sci.* **42**(1), 91–104 (2000), [http://dx.doi.org/10.1016/S0010-938X\(99\)00048-7](http://dx.doi.org/10.1016/S0010-938X(99)00048-7).
24. Y. C. Sica et al., "Atmospheric corrosion performance of carbon steel, galvanized steel, aluminium and copper in the North Brazilian Coast," *J. Braz. Chem. Soc.* **18**(1), 153–166 (2007), <http://dx.doi.org/10.1590/S0103-50532007000100017>.
25. Umwelt Bundes Amt, Schwefeldioxid-Emissionen, Available at <http://www.umweltbundesamt-daten-zur-umwelt.de/umweltdaten/public/theme.do?nodeIdent=3578> (15 July 2011).



Karolina Slamova received her MSc. degree in geography from the University of Freiburg in 2011. She is now employed at Fraunhofer ISE in the division 'photovoltaic modules, systems and reliability' and works on her PhD. at the University of Freiburg under the supervision of Professor Rüdiger Glaser. Her research interests include mapping of PV weathering stress factors by using geographical information systems (GIS), currently focussing on corrosion of PV modules and climate geo-data processing and analysis.



Rüdiger Glaser is professor with chair and director of the department of geography at the University of Freiburg. Previous academic positions include vice-dean of the faculty of forestry and environment in Freiburg (2004–2010), professor of geography (2001–2004) and senior lecturer (1991–2001) at the University of Heidelberg. He is a member of the Society of Canadian Studies and member of the supervisory board of the Geoinform AG. Since 2000, he is an elected member of the German Academy for Regional Studies (DAL). His research and teaching interests include climate change, global change, geocommunication and collaborative research environments.



Christian Schill received his diploma in physics in 1998 from the University of Freiburg, while working at Fraunhofer ISE on spectral response measurements of PV modules. He then worked both at the Freiburg materials research centre (FMF) and at the faculty of forest and environmental sciences, dealing with decision support systems and specializing on geo-data infrastructures. He then re-joined Fraunhofer ISE in 2008 and is now working on outdoor weathering of PV modules and climate geo-data.



Stefan Wiesmeier studied cartography, geomediatechnics and geoinformatics at the Munich University of applied sciences. From 2007 to 2010, he was employed as researcher at Fraunhofer ISE, where he focused on climate data processing and analysis and climate database development and durability analysis. Since 2010, he is member of a research group for applied and environmental geology at the University of Basel (Angewandte und Umweltgeologie, AUG) and holds in addition since 2011, a position at the department of applied econometrics of the University of Basel.



Michael Köhl obtained his diploma in physics in 1977 from the University of Stuttgart and his PhD in 2011 from the University of Hagen. He has been with Fraunhofer ISE since 1989 and is the head of the durability team in the division photovoltaic modules, systems and reliability. He currently works on service-life analyses with a focus on optical measurements and durability assessment. He has been the coordinator of many EU projects and leader of subtask 5 of the IP PERFORMANCE. He is the operating agent of task39 polymeric materials for solarthermal systems of the solar heating and cooling programme of the international energy agency.